A generic NLO SM framework for LHC and future collider processes

Pia Bredt [a,*]

[a]Department of Physics, University of Siegen,
Walter-Flex-Straße 3, 57068 Siegen, Germany

E-mail: pia.bredt@uni-siegen.de

In this talk I will present an automated framework calculating next-to-leading (NLO) corrections in the full Standard Model (SM) for arbitrary processes at hadron and lepton colliders. This framework is an element of the Monte-Carlo program WHIZARD simulating cross sections and differential distributions. The generalization of the implemented Frixione-Kunszt-Signer (FKS) scheme to systematically subtract QED and QCD infrared divergences in mixed coupling expansions will be discussed. Also, recent progress of the POWHEG-matched event generation and the inclusion of electroweak corrections in future lepton collider processes are subjects of this talk. In particular, results of our recent study will be shown applying electroweak (EW) corrections to multi-boson processes at a future multi-TeV muon collider.
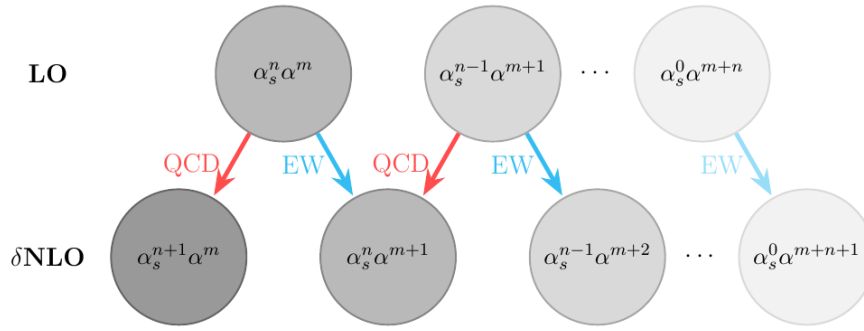
---

[*]Speaker

Figure 1: Connections of LO and NLO contributions to different coupling orders in a mixed coupling expansion.

1. Introduction

The automated inclusion of NLO SM corrections into collider physics simulations is a crucial element of Monte-Carlo event generators, which are able to make precise predictions for arbitrary processes. The NLO framework presented in this contribution builds on `WHIZARD` [1], a multi-purpose program for cross sections, differential distributions and simulated event samples for lepton- and hadron-collider experiments covering physics of the SM and beyond. It provides an intrinsic tree-level matrix element generator `O'Mega` [2] and a multi-channel phase-space integrator `VAMP` [3] with parallelization capabilities based on the Message Passing Interface (MPI) [4].

The implementation of the NLO module started with the automation of NLO QCD corrections [5–9], and has recently been extended to account for complete perturbative NLO corrections in the full SM [10, 11]. In this framework one-loop virtual matrix elements are accessed by generic interfaces to one-loop providers such as `OpenLoops` [12], `RECOLA` [13] and `GoSam` [14], and the FKS scheme [15] is chosen to subtract infrared singularities. The POWHEG matching scheme [16, 17] is an additional element implemented in `WHIZARD` to support the NLO QCD event generation matched to parton showers. This scheme is chosen as it works perfectly in conjunction with the FKS subtraction method. First work on this started with earlier studies on $e^+e^- \to t\bar{t}(H)$ precision calculations [18], and has recently been automated for e^+e^- and pp processes [7]. Other progress in the `WHIZARD`-code towards higher order contributions has lately been achieved with respect to an automated simulation of loop-induced processes with one-loop matrix elements from `OpenLoops`. The technical details on the automation of NLO SM corrections in `WHIZARD` and results of an application of NLO EW corrections to multi-boson processes at a future muon collider are summarized below.

2. The automation of NLO SM corrections in WHIZARD

The implementation of the NLO module in `WHIZARD` allows for a systematic cancellation of QCD and QED singularities – simultaneously, where needed – according to FKS subtraction. In this way, the complete tower of coupling order contributions at LO and NLO illustrated in Fig. 1 can be computed. In this regard, overlapping NLO QCD-EW contributions are also taken into account. Further essential ingredients of an automated computation of NLO EW corrections to

$pp \to t\bar{t}W^+$	$\alpha_s^n \alpha^m$	σ^{tot} [fb]		σ^{sig}
		MUNICH	WHIZARD	MUNICH-WHIZARD
LO_{21}	$\alpha_s^2 \alpha$	$2.411403(1) \cdot 10^2$	$2.4114(1) \cdot 10^2$	0.72
LO_{03}	α^3	$2.31909(1) \cdot 10^0$	$2.3193(1) \cdot 10^0$	1.76
δNLO_{31}	$\alpha_s^3 \alpha$	$1.18993(2) \cdot 10^2$	$1.1905(5) \cdot 10^2$	1.06
δNLO_{22}	$\alpha_s^2 \alpha^2$	$-1.09511(9) \cdot 10^1$	$-1.0947(3) \cdot 10^1$	1.13
δNLO_{13}	$\alpha_s \alpha^3$	$2.93251(3) \cdot 10^1$	$2.9334(8) \cdot 10^1$	1.14
δNLO_{04}	α^4	$5.759(3) \cdot 10^{-2}$	$5.756(4) \cdot 10^{-2}$	0.58

Table 1: Validation of fixed order cross section contributions to $pp \to t\bar{t}W^+$ at LO and NLO obtained with WHIZARD and MUNICH using OpenLoops with $\sigma^{\text{sig}} = |\sigma^{\text{tot}}_{\text{MUNICH}} - \sigma^{\text{tot}}_{\text{WHIZARD}}|/(\Delta^2_{\text{MUNICH}} + \Delta^2_{\text{WHIZARD}})$ where σ^{tot} denotes the total cross section and Δ the respective Monte-Carlo uncertainty.

LHC processes is the inclusion of photon-induced processes and the respective interrelation with the EW renormalization scheme.

For pure EW corrections dedicated cross-checks with MG5_aMC@NLO [19] for a set of benchmark processes at the LHC including neutral- and charged-current processes (with and without associated Higgs), VBF as well as single top plus jet processes are performed. With MUNICH/MATRIX [20–22] as reference tool, processes with on-shell bosons VV, VH, VVV, VVH and VHH with $V = W^\pm, Z$ at NLO EW as well as all α_s leading and subleading NLO contributions of $pp \to t\bar{t}(H/Z/W^\pm)$ are cross-validated. Exemplary, Tab. 1 shows comparisons of cross section contributions to $pp \to t\bar{t}W^+$ to all coupling orders at LO and NLO obtained with WHIZARD and MUNICH using OpenLoops. Due to $\sigma^{\text{sig}} \lesssim 2$ for the corresponding results, agreement could be achieved for relative MC errors well-below the per-mille level.

Processes with charged leptons and jets in the final state and an additional photon occurring at NLO EW require intricate IR-safety criteria including photon recombination and jet clustering. With the provision of appropriate phase-space cut evaluation requirements, WHIZARD supports the computation of NLO EW corrections to these processes. Cross-checks on cross sections at NLO EW for $pp \to e^+\nu_e j$ and $pp \to e^+e^- j$ in this respect have been performed with MG5_aMC@NLO.

For lepton-collider processes, NLO EW corrections in a fixed order massive initial-state approximation can be considered reliable under certain conditions of a collider setup. In this regard, initial-state masses and collider energies are preferred which yield small logarithms $\log m_l/\sqrt{s}$ originating from collinear initial-state photon radiation. WHIZARD supports this method with an adjusted FKS phase space construction for massive initial-state emitters and an improved interface to RECOLA. Cross-checks have been performed for $e^+e^- \to HZ$ at projected ILC energies and for $e^+e^- \to \mu^+\mu^-$ and $e^+e^- \to \tau^+\tau^-$ at $\sqrt{s} = 5$ and 7 GeV with reference results from MCSANCee [23, 24].

For all these above-mentioned validations of the NLO SM/EW automation in WHIZARD, explicit results and more details are listed in Ref. [10].

3. Application of NLO EW corrections to multi-boson processes at a muon collider

The NLO EW framework of WHIZARD is applied in our study to multi-boson processes at a multi-TeV muon collider, $\mu^+\mu^- \to V^n H^m$ with $V \in \{W^\pm Z\}$ and $n + m \leq 4$, for cross sections and

$\mu^+\mu^- \to X, \sqrt{s} = 3$ TeV	$\sigma_{\mathrm{LO}}^{\mathrm{incl}}$ [fb]	δ_{EW} [%]	δ_{ISR} [%]
W^+W^-	$4.6591(2) \cdot 10^2$	$+4.0(2)$	$+13.82(4)$
ZZ	$2.5988(1) \cdot 10^1$	$+2.19(6)$	$+15.71(4)$
HZ	$1.3719(1) \cdot 10^0$	$-1.51(4)$	$+30.24(3)$
W^+W^-Z	$3.330(2) \cdot 10^1$	$-22.9(2)$	$+2.90(9)$
W^+W^-H	$1.1253(5) \cdot 10^0$	$-20.5(2)$	$+7.10(8)$
ZZZ	$3.598(2) \cdot 10^{-1}$	$-25.5(3)$	$+5.24(8)$
HZZ	$8.199(4) \cdot 10^{-2}$	$-19.6(3)$	$+8.39(8)$
HHZ	$3.277(1) \cdot 10^{-2}$	$-25.2(1)$	$+7.58(7)$
$W^+W^-W^+W^-$	$1.484(1) \cdot 10^0$	$-33.1(4)$	$-1.3(1)$
W^+W^-ZZ	$1.209(1) \cdot 10^0$	$-42.2(6)$	$-1.8(1)$
W^+W^-HZ	$8.754(8) \cdot 10^{-2}$	$-30.9(5)$	$-0.1(1)$
W^+W^-HH	$1.058(1) \cdot 10^{-2}$	$-38.1(4)$	$+1.7(1)$
$ZZZZ$	$3.114(2) \cdot 10^{-3}$	$-42.2(2)$	$+0.8(1)$
$HZZZ$	$2.693(2) \cdot 10^{-3}$	$-34.4(2)$	$+1.4(1)$
$HHZZ$	$9.828(7) \cdot 10^{-4}$	$-36.5(2)$	$+2.2(1)$
$HHHZ$	$1.568(1) \cdot 10^{-4}$	$-25.7(2)$	$+5.7(1)$

Table 2: LO cross sections of multi-boson production at a $\mu^+\mu^-$ collider for $\sqrt{s} = 3$ TeV with relative correction factors $\delta_{\mathrm{EW}} = \sigma_{\mathrm{NLO}}^{\mathrm{incl}}/\sigma_{\mathrm{LO}}^{\mathrm{incl}} - 1$ and $\delta_{\mathrm{ISR}} = \sigma_{\mathrm{LO,LL\text{-}ISR}}^{\mathrm{incl}}/\sigma_{\mathrm{LO}}^{\mathrm{incl}} - 1$.

distributions at NLO EW [11]. Due to the large initial-state masses of a $\mu^+\mu^-$ collider compared to e^+e^- collider concepts, a fixed $\mathcal{O}(\alpha)$ expansion, keeping the masses explicit in the matrix elements, is a viable approximation. Parametrically, the leading logarithmic term beyond NLO would be of order $(\alpha/\pi)^2 \log^2(Q^2/m^2) \sim 0.1\%$, and thus negligible for the scope of our study. One-loop EW virtual contributions are provided by RECOLA accounting for the full mass dependence of fermions and bosons.

In Tab. 2, total cross sections for two-, three- and four-boson production at a 3-TeV muon collider are shown with $\delta_{\mathrm{EW}} = \sigma_{\mathrm{NLO}}^{\mathrm{incl}}/\sigma_{\mathrm{LO}}^{\mathrm{incl}} - 1$ denoting the relative correction of the NLO EW with respect to the corresponding LO result. These factors feature a suppression of NLO with respect to LO cross sections growing in size with the number of bosons in the final state. This can be explained mostly by the negatively contributing EW Sudakov logarithms in the high-energy regime. In addition, radiative return effects due to hard photon radiation lead to positive enhancements. This QED effect especially plays a role for a small number of final-state bosons with pronounced thresholds. This is additionally reflected by the factor $\delta_{\mathrm{ISR}} = \sigma_{\mathrm{LO,LL\text{-}ISR}}^{\mathrm{incl}}/\sigma_{\mathrm{LO}}^{\mathrm{incl}} - 1$ displayed in the last column of Tab. 2 which decreases with the number of final-state bosons. It is defined by the relative correction of applying leading-logarithmic (LL) electron PDFs for collinear initial-state radiation (ISR) with respect to the pure LO cross section.

Another focus was on the large suppression factors of (multi-)Higgsstrahlung with respect to other processes at high energy scales, e. g. at 10 and 14 TeV, shown in corresponding tables in Ref. [11]. Differential distributions for $\mu^+\mu^- \to HZ$ for this reason have been studied from which a selection, i. e. cross sections differential in the Higgs polar angle θ_H, is presented in Fig. 2. Besides the distribution for the Born component, two NLO curves, for which one includes a cut on hard photons of $E_\gamma < 0.7\sqrt{s}/2$, are shown for comparison for two different energies, $\sqrt{s} = 3$ and 14 TeV. As it is
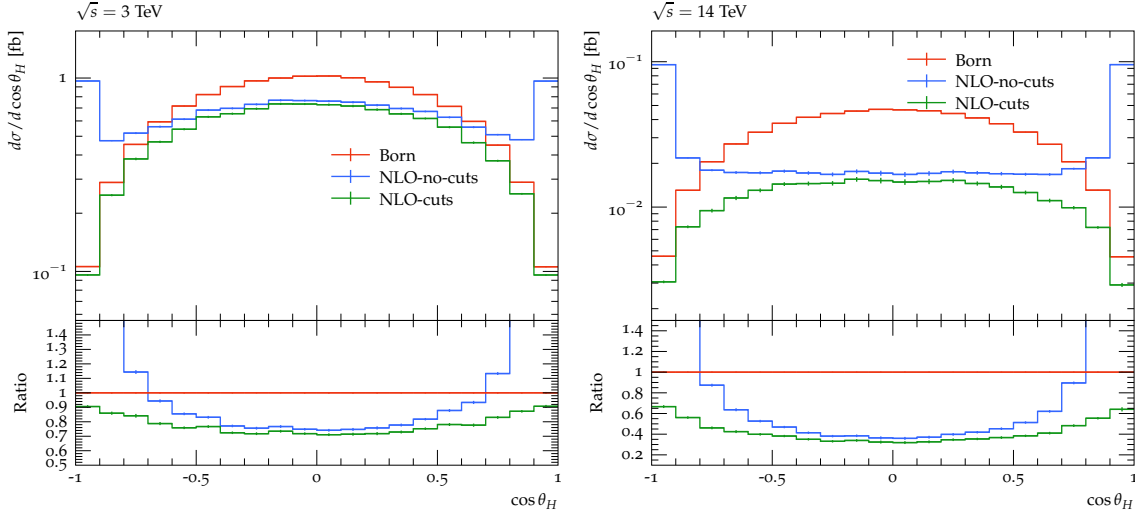
Figure 2: Fixed-order differential distributions of the Higgs polar angle $d\sigma/d\cos\theta_H$ for $\mu^+\mu^- \to HZ$ at $\sqrt{s} = 3$ TeV (left) and $\sqrt{s} = 14$ TeV (right) with 'NLO-cuts' describing the distribution at NLO combined with a cut on hard photons $E_\gamma < 0.7\sqrt{s}$ and 'NLO-no-cuts' the NLO distribution without this cut, respectively.

typical for Higgsstrahlung due to its s-channel like nature, the bulk of the Born cross section comes from the central part of the angular range. While the real emission part at NLO contributes mostly at small angles of the Higgs with respect to the beam axis due to hard photon radiation, the negatively contributing virtual component is dominant at NLO in the central part. In fact, the suppression factor of the NLO with respect to the Born distribution at $\theta_H = 90°$ is approximated very well by the corresponding NLL EW Sudakov form factor as shown in our study. This kinematic separation of pure QED with respect to EW virtual effects at NLO in α is very specific for Higgsstrahlung.

4. Conclusions & Outlook

The automated NLO SM framework of `WHIZARD` is functional and validated for a broad set of processes at hadron and lepton colliders. In our study, applying this framework to muon collider physics, EW corrections turn out to have the highest significant effect for high boson multiplicities and high collider energies, which is caused by large EW Sudakov logarithms. Future plans include the application of NLO-NLL electron PDFs [25, 26] in LO and NLO lepton collider physics simulations with `WHIZARD`. Efficiency improvements on the NLO framework, essentially including the extension of the implemented resonance-aware FKS scheme to pp processes, are being developed. Furthermore, simulations of NLO observables using SMEFT operators are targeted, where recent progress has been achieved on the `WHIZARD+GoSam` interface using UFO models.

Acknowledgements

MUNICH, Jonas Lindert for support with `OpenLoops` and Marius Höfer for help improving the `WHIZARD+GoSam` interface.

References

[1] W. Kilian, T. Ohl and J. Reuter, Eur. Phys. J. C **71** (2011), 1742, arXiv: 0708.4233 [hep-ph].

[2] M. Moretti, T. Ohl and J. Reuter, arXiv: hep-ph/0102195 [hep-ph].

[3] T. Ohl, Comput. Phys. Commun. **120** (1999), 13-19, arXiv: hep-ph/9806432 [hep-ph].

[4] S. Brass, W. Kilian and J. Reuter, Eur. Phys. J. C **79** (2019) no.4, 344, arXiv: 1811.09711 [hep-ph].

[5] C. Weiss, Top quark physics as a prime application of automated higher-order corrections, PhD thesis, Hamburg U., Hamburg, 2017.

[6] V. Rothe, Automation of NLO QCD Corrections and the Application to *N*-Jet Processes at Lepton Colliders, PhD thesis, Hamburg U., Hamburg, 2021.

[7] P. Stienemeier, Automation and Application of fixed-order and matched NLO Simulations, PhD thesis, Hamburg U., Hamburg, 2022.

[8] F. Bach, B. C. Nejad, A. Hoang, W. Kilian, J. Reuter, M. Stahlhofen, T. Teubner and C. Weiss, JHEP **03** (2018), 184, arXiv: 1712.02220 [hep-ph].

[9] B. Chokoufé Nejad, W. Kilian, J. M. Lindert, S. Pozzorini, J. Reuter and C. Weiss, JHEP **12** (2016), 075, arXiv: 1609.03390 [hep-ph].

[10] P. M. Bredt, Automated NLO Electroweak Corrections to Processes at Hadron and Lepton Colliders, PhD thesis, Hamburg U., Hamburg, 2022.

[11] P. M. Bredt, W. Kilian, J. Reuter and P. Stienemeier, JHEP **12** (2022), 138, arXiv: 2208.09438 [hep-ph].

[12] F. Buccioni, J. N. Lang, J. M. Lindert, P. Maierhöfer, S. Pozzorini, H. Zhang and M. F. Zoller, Eur. Phys. J. C **79** (2019) no.10, 866, arXiv: 1907.13071 [hep-ph].

[13] S. Actis, A. Denner, L. Hofer, A. Scharf and S. Uccirati, JHEP **04** (2013), 037, arXiv: 1211.6316 [hep-ph].

[14] G. Cullen, *et al.* Eur. Phys. J. C **74** (2014) no.8, 3001, arXiv: 1404.7096 [hep-ph].

[15] S. Frixione, Z. Kunszt and A. Signer, Nucl. Phys. B **467** (1996), 399-442, arXiv: hep-ph/9512328 [hep-ph].

[16] P. Nason, JHEP **11** (2004), 040, arXiv: hep-ph/0409146 [hep-ph].

[17] S. Frixione, P. Nason and C. Oleari, JHEP **11** (2007), 070, arXiv: 0709.2092 [hep-ph].

[18] B. Chokoufe Nejad, W. Kilian, J. Reuter and C. Weiss, PoS **EPS-HEP2015** (2015), 317, arXiv: 1510.02739 [hep-ph].

[19] R. Frederix, S. Frixione, V. Hirschi, D. Pagani, H. S. Shao and M. Zaro, JHEP **07** (2018), 185, arXiv: 1804.10017 [hep-ph].

[20] S. Kallweit, J. M. Lindert, P. Maierhöfer, S. Pozzorini and M. Schönherr, JHEP **04** (2015), 012, arXiv: 1412.5157 [hep-ph].

[21] L. Buonocore, M. Grazzini, S. Kallweit, C. Savoini and F. Tramontano, Phys. Rev. D **103** (2021), 114012, arXiv: 2102.12539 [hep-ph].

[22] R. Bonciani, L. Buonocore, M. Grazzini, S. Kallweit, N. Rana, F. Tramontano and A. Vicini, Phys. Rev. Lett. **128** (2022) no.1, 012002, arXiv: 2106.11953 [hep-ph].

[23] R. R. Sadykov, *et al.* J. Phys. Conf. Ser. **1525** (2020) no.1, 012012

[24] A. Arbuzov, S. Bondarenko, Y. Dydyshka, L. Kalinovskaya, L. Rumyantsev, R. Sadykov, V. Yermolchyk and U. Yermolchyk, JETP Lett. **116** (2022) no.4, 199-204, arXiv: 2206.09469 [hep-ph].

[25] S. Frixione, JHEP **11** (2019), 158, arXiv: 1909.03886 [hep-ph].

[26] V. Bertone, M. Cacciari, S. Frixione and G. Stagnitto, JHEP **03** (2020), 135, arXiv: 1911.12040 [hep-ph].